

We are IntechOpen, the world's leading publisher of Open Access books Built by scientists, for scientists

6,400

Open access books available

174,000

International authors and editors

190M

Downloads

Our authors are among the

154

Countries delivered to

TOP 1%

most cited scientists

12.2%

Contributors from top 500 universities



WEB OF SCIENCE™

Selection of our books indexed in the Book Citation Index
in Web of Science™ Core Collection (BKCI)

Interested in publishing with us?
Contact book.department@intechopen.com

Numbers displayed above are based on latest data collected.
For more information visit www.intechopen.com



Chapter

On-Chip Sub-Diffraction THz Spectroscopy of Materials and Liquids

Randy M. Sterbentz and Joshua O. Island

Abstract

This chapter summarizes the trends in terahertz measurements on the surface of rigid and flexible substrates. It focuses on research incorporating fast photoconductive switches to generate and detect on-chip THz pulses using a femtosecond laser. The chapter aims to review progress toward the study of picosecond dynamics and THz spectroscopy of materials and liquids. We emphasize general sub-diffraction techniques for THz spectroscopy, transmission line and waveguide design considerations, time-domain measurements for studies of material dynamics, and provide a survey of recent research on the THz spectroscopy of materials and liquids on-chip. We conclude with an outlook on the field and highlight promising new directions. This chapter is meant to be an introduction and a general guide to this emerging field for new researchers interested in on-chip THz studies.

Keywords: on-chip, terahertz, spectroscopy, materials, liquids

1. Introduction

Terahertz (THz) time-domain spectroscopy has led to a deeper understanding of the properties of matter. Developed from early measurements of the optical switching of silicon [1, 2], generation and detection of free-space THz pulses in the late 1980s [3–5] gave way to a new spectroscopic approach for fundamental science [6]. With both amplitude and phase sensitivity, the technique allows direct extraction of the complex-valued index of refraction. The THz spectrum covers a window of energies (and timescales) that host rich phenomena in solids including: important carrier dynamics [7, 8], charge ordering [9], gapped excitations in superconductors [8, 10], magnetic excitations and dynamics [11], and energy quantization in the quantum Hall effect [12–14].

THz radiation has a number of appealing properties for biomedical sciences as well [15–19]. The non-ionizing and non-destructive nature of the radiation makes it particularly promising for non-invasive, *in vivo* imaging and cancer detection [20–22].

The time resolution of time-domain measurements opens the door to studying important hydration dynamics in solvated biomolecules and chemical reactions at the picosecond timescale [23]. Moreover, the capacity of this frequency of radiation to resonantly excite intra- and inter-molecular oscillations presents a unique advantage in the detection of low-concentration biomolecules. Highlighting a few notable recent examples, Cheon et al. showed that methylated DNA presents a resonant excitation at 1.6 THz and the degree of methylation can be quantified by the amplitude of the absorption peak [24]. Niessen et al. have reported clear resonant features of lysozyme, *E. coli* DHFR, and RNA G-quadruplex [25].

While the majority of research involving THz spectroscopy has been done using free-space radiation, there is a growing interest in probing samples smaller than the diffraction limit on the surface of a chip. The diffraction limit puts a fundamental restriction on the smallest size of a probed sample at roughly the half-wavelength ($\lambda/2$) [26, 27]. Since THz radiation has wavelengths on the order of a millimeter, this limit impedes THz spectroscopy of microscopic samples such as high-quality exfoliated two-dimensional (2D) flakes with lateral dimensions on the order of tens of microns. Two-dimensional materials have enjoyed fantastic appeal in material and applied sciences since the exfoliation and isolation of a single layer of carbon atoms [28]. The recent observation of unconventional superconductivity in two layers of graphene precisely rotated by 1.1 degrees [29, 30] has reinvigorated investigations of correlated phenomena in these heterostructures. Near-field techniques have been developed to overcome the diffraction limit using apertures and sharp metal tips, but another promising direction is the use of on-chip waveguides and transmission lines to perform THz measurements on micrometer samples.

Sub-diffraction techniques have also revolutionized biotechnology. The zero mode waveguide presents a canonical example, now allowing researchers to perform single-molecule measurements at biologically relevant concentrations all at exceedingly small sample sizes [31, 32]. This is generally achieved by reducing the observation space to a sub-diffraction aperture of zeptoliter volume, allowing rapid and parallel measurements of single molecules at micromolar concentrations [33]. Researchers are actively trying to extend sub-diffraction techniques to the terahertz region of the electromagnetic spectrum for fingerprint analysis of bioliquids. This is challenging as water leads to strong attenuation of THz signals. For the same reason that THz radiation is appealing for identifying biomolecules, water molecules themselves present strong resonant absorptions. These absorptions mask the underlying fingerprints of the biomolecules present in a liquid sample. In Cheon et al., measurements of methylated DNA are performed at 253 K (-20°C) in order to freeze liquid water and reduce background absorption [24]. In Niessen et al. paraffin oil is used to maintain protein hydration in place of water [25]. Confining small amounts of bioliquids in microfluidic cells on the surface of on-chip THz spectrometers allows a reduction of the interaction volume between the probing field and the target sample and may provide avenues to diagnostic devices.

This chapter is organized into seven sections including this introduction. Section 2 provides a survey of the historical developments in sub-diffraction techniques for THz measurements. Section 3 presents waveguide and transmission line design considerations for on-chip measurements. Section 4 surveys research on time-domain measurements for studies of dynamics in material systems. Section 5 reviews research on THz spectroscopy on-chip and examples of spectroscopy of materials. Section 6 reviews research on THz spectroscopy of liquids. Finally, Section 7 concludes the chapter and provides an outlook on the field.

2. Historical summary of sub-diffraction techniques

Sub-diffraction techniques have been successfully used in THz imaging and microscopy, whereas sub-diffraction has proven to be more challenging [34]. Many interesting physical systems have geometries smaller than the diffraction limit: a scale less than half the wavelength of radiation where light does not interact efficiently with a material. This limit for THz radiation is on the order of $100\ \mu\text{m}$. In order to probe materials below the diffraction limit, several techniques have been developed which can be grouped into two general areas: apertures and sharp metal tips. See **Figure 1** for simple model representations of these two approaches.

Apertures form the earliest examples of sub-diffraction imaging and the idea dates back to suggestions by Synge in 1928 [37]. Aperture techniques for THz radiation were experimentally realized as early as 1993 when Merz et al. displayed an increased resolution of $\lambda/2$ [38]. Researchers have continued to improve signal resolution [39–43], up to a recent publication by Kawano, et al. where they demonstrated a $9\ \mu\text{m}$ resolution using an aperture on a gallium arsenide-aluminum gallium arsenide (GaAs/AlGaAs) substrate [35]. **Figure 1(a-b)** display their device. The THz radiation is enhanced by the near-field probe and detected using the buried 2D electron gas (2DEG), as shown schematically in **Figure 1(b)**. The aperture approach is limited by the cut-off effect: as the aperture becomes smaller, and the resolution better, the transmitted signal is reduced and the signal-to-noise ratio (SNR) ultimately suffers [44, 45]. As an inconvenient technicality, the detector must be exceedingly close to the aperture to prevent signal loss from quick divergence of the radiation through the aperture.

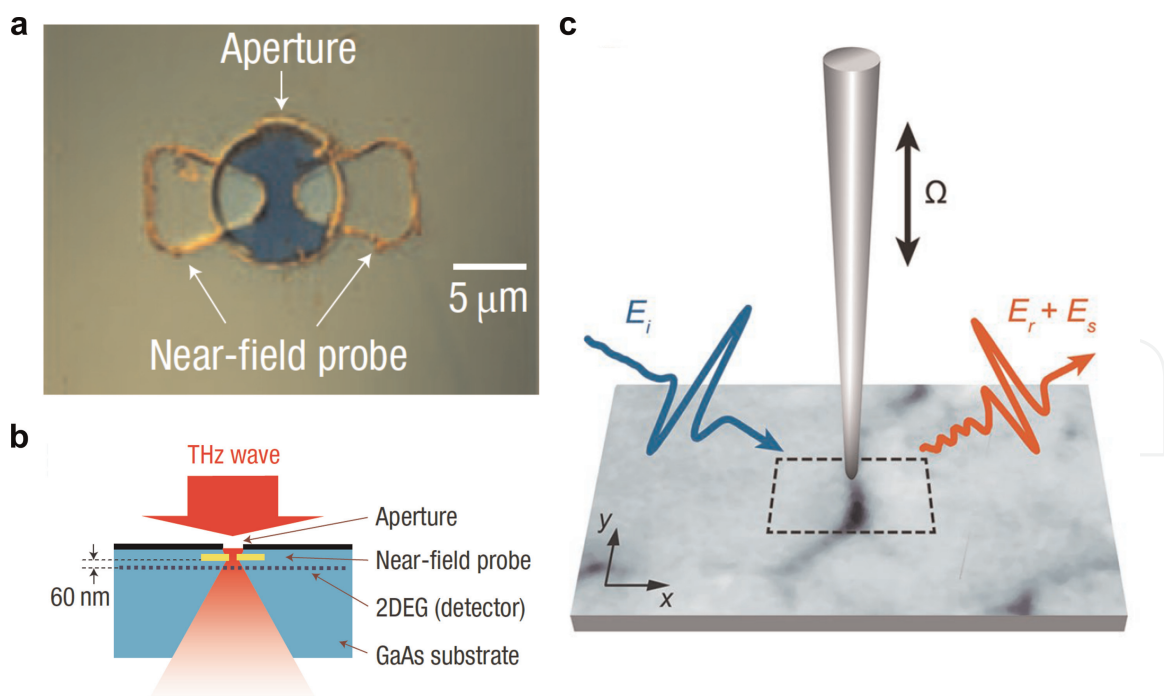


Figure 1. Sub-diffraction terahertz imaging and spectroscopy techniques. (a) Aperture-based techniques limit the probing radiation to a small aperture, thereby increasing the resolution. This is a recent example from Kawano et al. showing an optical image of an aperture on the surface of a GaAs substrate. (b) Model schematic of the aperture device and principle of operation. The THz radiation is enhanced at the near-field probe and detected with the buried 2DEG. Panels (a) and (b) have been adapted from ref. [35]. (c) Near-field imaging and spectroscopy with a sharp metal tip. This is an example from Moon et al. showing the principle of operation. THz radiation is scattered off the metal tip and detected. Panel (c) has been adapted from ref. [36].

A second approach involves the use of a metal tip that enhances the probing field through near-field, plasmonic effects [46–49]. This was demonstrated in 1985 by Wessel using infrared radiation [46] and subsequently investigated with THz radiation [36, 47–49]. An example of this technique is shown in **Figure 1(c)**. The confinement at the apex of the metal tip produces strongly enhanced fields and sub-diffraction radiation. The increased resolution is comparable to the tip diameter (tens of nanometers). This technique has enjoyed recent interest in the imaging of 2D materials at THz frequencies [50, 51]. The technique has a few drawbacks. One, a probing field is required which may also perturb the sample under study and, two, the tip itself can lead to unwanted tip-sample interactions. Moreover, most of the scattered signal from the sample surface is background signal and the weak tip enhanced radiation requires long measurement times. Ribbek et al. have reported detection of the near-field part of the scattered signal with an integration time of 19 mins for a scan delay of 7.35 ps (amounting to a frequency resolution of 0.14 THz) [52].

Lastly, on-chip waveguides and transmission lines can be used to confine sub-diffraction radiation [53–56]. To perform spectroscopy, photoconductive switches can be fabricated near or within the on-chip circuit to generate and sample single cycle pulses using a femtosecond laser. This measurement scheme is similar to the early studies by Auston et al. that were the basis of free-space spectroscopy but that were abandoned due to pulse attenuation from lossy substrates [2]. With careful design, waveguides and transmission lines can be fabricated to achieve reflection-free spectroscopy resulting in long time-domain scans and high frequency resolution.

3. Circuit design considerations

Ultrafast pulse generation and readout on-chip have been accomplished using a number of transmission line and waveguide designs. In the earliest studies from Auston and colleagues, the chips were fabricated with microstrip lines on high-resistivity silicon [1, 57, 58]. Following this, two and three-arm coplanar transmission lines were investigated as well as coplanar waveguides [59–66]. More recently, single conductor waveguides (Goubau lines) have been used to route THz radiation and single pulses on chip [67–71]. In most cases, the circuits have been fabricated using conventional metals, but superconductors have also been used [72].

An overview of these different designs is shown in **Figure 2**. **Figure 2(a)** shows the original design by Auston [1]. The geometry consists of a continuous ground plane on the back of a silicon substrate and a hundreds-of-microns wide stripline on the surface of the chip. Auston used this design to demonstrate ultrafast (picosecond) switching of electrical signals on-chip with the aid of optical laser pulses to electrically open and close microstrip gaps. Shortly after this, Ketchen et al. measured picosecond pulses in a three arm transmission line [59]. A schematic of this design is shown in **Figure 2(b)**. Aluminum lines (5 microns wide) were patterned using standard photolithographic techniques on top of a silicon-on-sapphire wafer. The silicon was subsequently radiation-damaged to produce short (less than 1 ps) carrier lifetimes required for pulse generation and detection with a femtosecond (80 fs) laser. Using this design, the authors were able to change the relative distance between the locations of the pulse generation and detection to measure pulse dispersion. They found that the pulse width increased roughly 1 ps for a propagation length of 8 mm. **Figure 2(c)** shows an example of a coplanar waveguide design studied in ref. [70]. Here, a ground plane surrounds a center conductor and electrical lines for connections to the photoconductive switches.

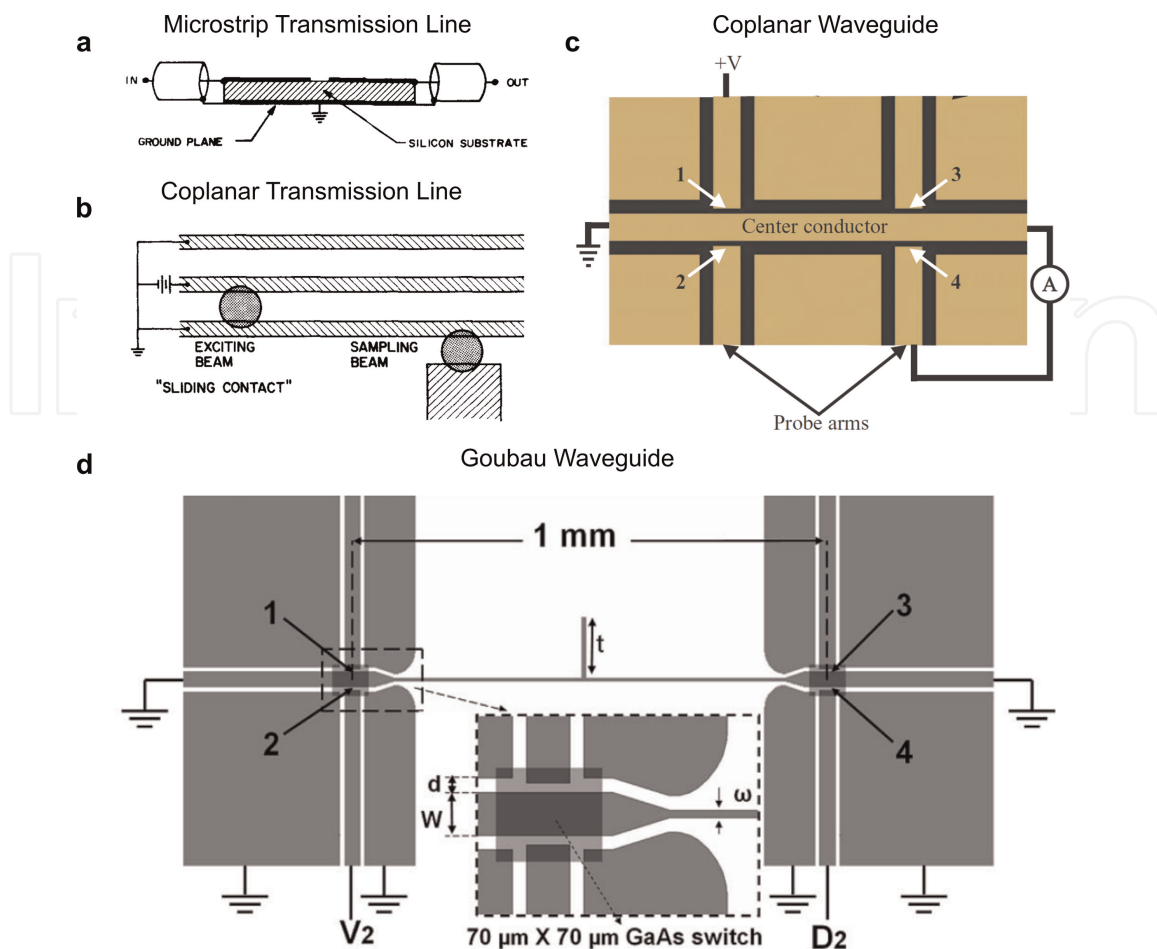


Figure 2. Various transmission line and waveguide designs for on-chip THz studies. (a) An example of a microstrip line design. This schematic shows a side view of the device. A single conductor (hundreds of microns wide) is photolithographically patterned on top of the silicon substrate. The back side is coated with metal to function as a ground plane. This panel has been adapted from ref. [1]. (b) An example of a coplanar transmission line design. Two grounded lines surround a center conductor. Readout (sampling) is accomplished with a fourth electrical line at the bottom. This panel has been adapted from ref. [59]. (c) An example of a coplanar waveguide design. A center conductor is surrounded by ground plane patches and readout is performed with additional electrical lines (labeled probe arms). This panel has been adapted from ref. [66]. (d) An example of a Goubau (single conductor) waveguide. A single metallic strip connects two sides of the device used for pulse generation and readout. It also includes a stub filter along the transmission line of length l to create a band-stop filter. This panel has been adapted from ref. [70].

The circuit is created using a photolithographically defined mask and deposition of titanium (10 nm) and gold (200 nm) metals. The circuit is patterned on a gallium arsenide substrate with low temperature grown gallium arsenide (LT-GaAs) of 2 microns thickness used as photoconductive switches. The last example is a single conductor Goubau line as shown in **Figure 2(d)** from ref. [70]. Here, the single conductor from a coplanar design, such as that shown in **Figure 2(c)**, is extended across the chip without an adjacent ground plane. Dazhang et al. fabricated this structure on top of a quartz substrate using LT-GaAs as photonconductive switches.

All of these designs, in principle, can accommodate a microfluidic cell placed on top of the chip to hold small amounts of bioliquids for study. Several groups have incorporated such cells for studies of liquid analytes [73–81].

There are a few particularly attractive features of using these types of circuits fabricated on-chip. Photolithographically-defined electrodes allow control over where the radiation is routed. This includes fabricating various bends and branches to guide and even split the radiation along different paths [82]. Moreover, waveguide modes

can be selectively excited. Wu et al. has shown that the dominant modes in a coplanar waveguide, slotline and coplanar modes, can be selectively excited using two photoconductive switches and a defocused laser spot [65]. This is advantageous because the field orientations for the two modes are different and one may couple better to a material or bioliquid under study. This was exactly the case in Wu et al.'s study as they found that the coplanar mode coupled better to their sample than the slotline mode. Follow up full wave modeling supported this experimental result, finding that decoupling the gate line from the ground plane better coupled the waveguide modes to the plasmon modes [83]. In such a way, the general electric field orientation can be controlled with careful choice of circuit design. For example, the coplanar transmission line design predominantly displays fields horizontal to the chip surface for materials placed between the lines. The Goubau line presents a vertical electric field for materials placed on top of the conductor. In this way, a preferential direction of the electric field excitation can be chosen.

As can be readily surmised, attenuation and pulse dispersion become significant factors in on-chip studies. As opposed to free space measurements, the pulsed radiation on-chip travels through lossy media. There are three considerations to improve the bandwidth for on-chip measurements. The first and most important is by judicious choice of a low loss substrate. Several materials have been investigated as low loss THz substrates and windows including sapphire, quartz, polyethylene, picarin, polytetrafluoroethylene (PTFE), and polyethylene terephthalate (PET) [63, 84–88]. On-chip bandwidths greater than 2 THz have been realized using picarin (Tsurupica) [63]. Another method to improve bandwidth is by thinning the substrate so the effective permittivity is lowered [89, 90]. Picarin may not support aggressive thinning ($< 100 \mu\text{m}$) required for appreciable improvement but quartz is a promising alternative [89, 90]. The last method is to optimize the pulse generation and detection. The generated electric field of the THz pulse is proportional to the transient photocurrent density in the semiconducting junction [91, 92],

$$E_{\text{THz}} \propto \frac{\partial J}{\partial t} = e \left(n \frac{\partial v_n}{\partial t} + v_n \frac{\partial n}{\partial t} + p \frac{\partial v_p}{\partial t} + v_p \frac{\partial p}{\partial t} \right), \quad (1)$$

where J is the photocurrent density, n and p are the respective electron and hole carrier densities, and v_n and v_p are the respective electron and hole average velocity. The rate of change of the densities is related to the relaxation time of the semiconducting material (τ_m) and the pulse width of the excitation laser (Δt),

$$\frac{dn}{dt} = -\frac{n}{\tau_m} + n_0 \exp - (t/\Delta t)^2, \quad (2)$$

where n_0 is the carrier density at $t = 0$ s. The same equation applies for the hole carrier density. The rate of change of the velocity is proportional to the applied electric field (E) (the voltage bias applied to the junction) through,

$$\frac{dv_{n,p}}{dt} = -\frac{v_{n,p}}{\tau_s} + \frac{q_{n,p}}{m_{n,p}} E, \quad (3)$$

where τ_s is the momentum relaxation rate and $m_{n,p}$ is the effective mass for electrons and holes respectively. Summarizing these relations, there are two aspects that will improve signal and bandwidth. The first is by using a material with a fast

carrier relaxation rate and the second is utilizing a laser with a short pulse width. Radiation damaged silicon has a relaxation time of 560 fs [93] but shorter relaxation rates have been observed in LT-GaAs (≈ 300 fs) [94].

4. Ultrafast pulse measurements

Besides spectroscopy, ultrafast pulse measurements can be used to study carrier relaxation times, magnetization dynamics, and hydration processes in the time domain. Strictly speaking, these include studies that are not interested in the frequency domain and focus solely on the time-domain data.

Some of the earliest examples harness on-chip pulses to study ballistic transport in clean one-dimensional and two-dimensional systems [95, 96]. Shaner and Lyon studied two-dimensional electron gas (AlGaAs/GaAs) structures connected to an on-chip coplanar waveguide [95]. From their THz time-domain data, shown in **Figure 3(a)**, resonant oscillations appear for positive magnetic fields after a 50 ps time delay. **Figure 3(b)** displays their full data, showing the evolution of collector voltage as a function of magnetic field and time delay. The ballistic signal is distinguished by a stable signal over time (horizontal streaks), and signatures of magnetoplasmon oscillations in the 2DEG are evident by the weak signal modulation with magnetic field. Zhong et al. performed a similar experiment with carbon nanotubes connected to an on-chip coplanar transmission line [96]. They also observed ballistic carrier resonances in their time-domain data, **Figure 3(c)**, that change with the length (L_g) of the ballistic channel.

The largest category of these investigations includes emission studies of various materials including GaAs [64], InAs nanowires [98], topological insulators [99–101], silicon [102], graphene [71, 93, 97, 103, 104], molybdenum disulfide [105], carbon nanotubes [106], GaAs nanowires [107], and field emission in nanojunctions [108]. Hunter et al. demonstrated emission of picosecond pulses from graphene flakes attached to an on-chip Goubau waveguide, **Figure 3(d)** [71]. The amplitude of the pulse could be linearly controlled with the applied bias to the graphene junction (inset of **Figure 3(d)**). Using circularly polarized light, McIver et al. showed that helicity-dependent picosecond photocurrents could be measured in graphene junctions using on-chip Goubau waveguides. **Figure 3(e)** displays the data showing that the measured photocurrent changes sign when the bias direction is changed across the graphene.

Ultrafast on-chip pulses have also been used to study picosecond switching dynamics in magnets and strained semiconductors [109–116]. Of particular note, Gerrits et al. studied magnetization reversal in permalloy films (NiFe) [109]. They showed that by using two photoconductive switches to shape ultrafast pulses to excite the material, they could suppress unwanted ringing effects with a second stop pulse. Yang et al., using a coplanar transmission line, displayed magnetization reversal in GdFeCo films with 10 ps pulses [113]. The mechanism proposed for the switching is heating caused by the electrical pulses. Interestingly, only 4 fJ of energy is required to switch a 20 nm³ magnetic cell.

5. THz spectroscopy on-chip

Using two photoconductive switches fabricated close to a transmission line or waveguide on-chip, it is possible to perform spectroscopy from the time-domain data

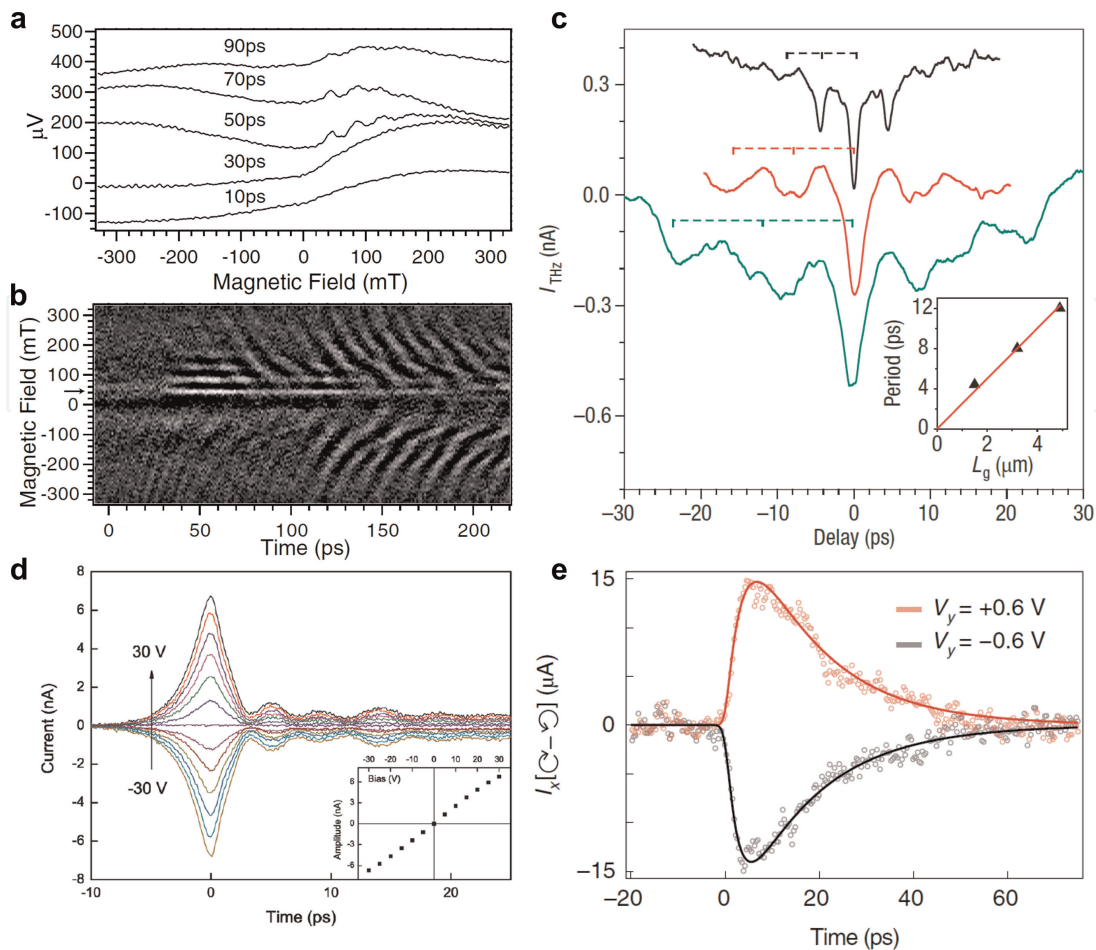


Figure 3.

Time-domain studies of various materials. (a) Ballistic carrier transport in a two-dimensional electron gas (2DEG). The collector voltage (y-axis) is plotted as a function of perpendicular magnetic field for different time delays between the generation switch and collector. Oscillations corresponding to ballistic transport can be seen for delays of 50 ps and greater. (b) Collector voltage plotted as a function of magnetic field and time delay. Horizontal streaks in the data correspond to ballistic transport and weaker oscillations are from magnetoplasmon excitations. Panels (a) and (b) have been adapted from ref. [95]. (c) Drain current of a carbon nanotube device as a function of time delay between two on-chip THz pulses. Dips in the data correspond to ballistic carrier transport. The curves from top to bottom correspond to ballistic channels with lengths of $L_g = 1.5$ mm (black), 3.2 mm (red) and 4.9 mm (green). This panel has been adapted from ref. [96]. (d) Readout current as a function of time delay between generation and detection pulses for a graphene junction emission switch. The various curves correspond to different voltage biases applied to the graphene flake. This panel has been adapted from ref. [71]. (e) Helicity-dependent photocurrent as a function of time delay between excitation pulse and readout pulse. The two curves show that the photocurrent changes sign for different orientations of the applied voltage bias, as expected for anomalous hall currents. This panel has been adapted from ref. [97].

using either pulsed lasers or continuous wave optical beating. Several research groups have investigated circuit elements that lead to resonant features in the THz spectrum. For example, Dazhang et al. have used a Goubau waveguide with a stub line, shown in **Figure 2(d)**, to create a band-stop filter [70]. **Figure 4(a)** displays their data showing the measured time-domain scan in the inset and the Fourier transformed data in the main panel. Band-stop response can be seen at the location of the arrows centered at 250 GHz (fundamental mode) and 780 GHz (third harmonic).

Very recently, Yoshioka et al. have demonstrated on-chip spectroscopy using continuous wave THz radiation created from the optical beating of two near-IR lasers [117]. This technique offers greater frequency resolution (10 MGz vs. 10 GHz) when compared with the time-domain technique. **Figure 4(b)** displays data from their

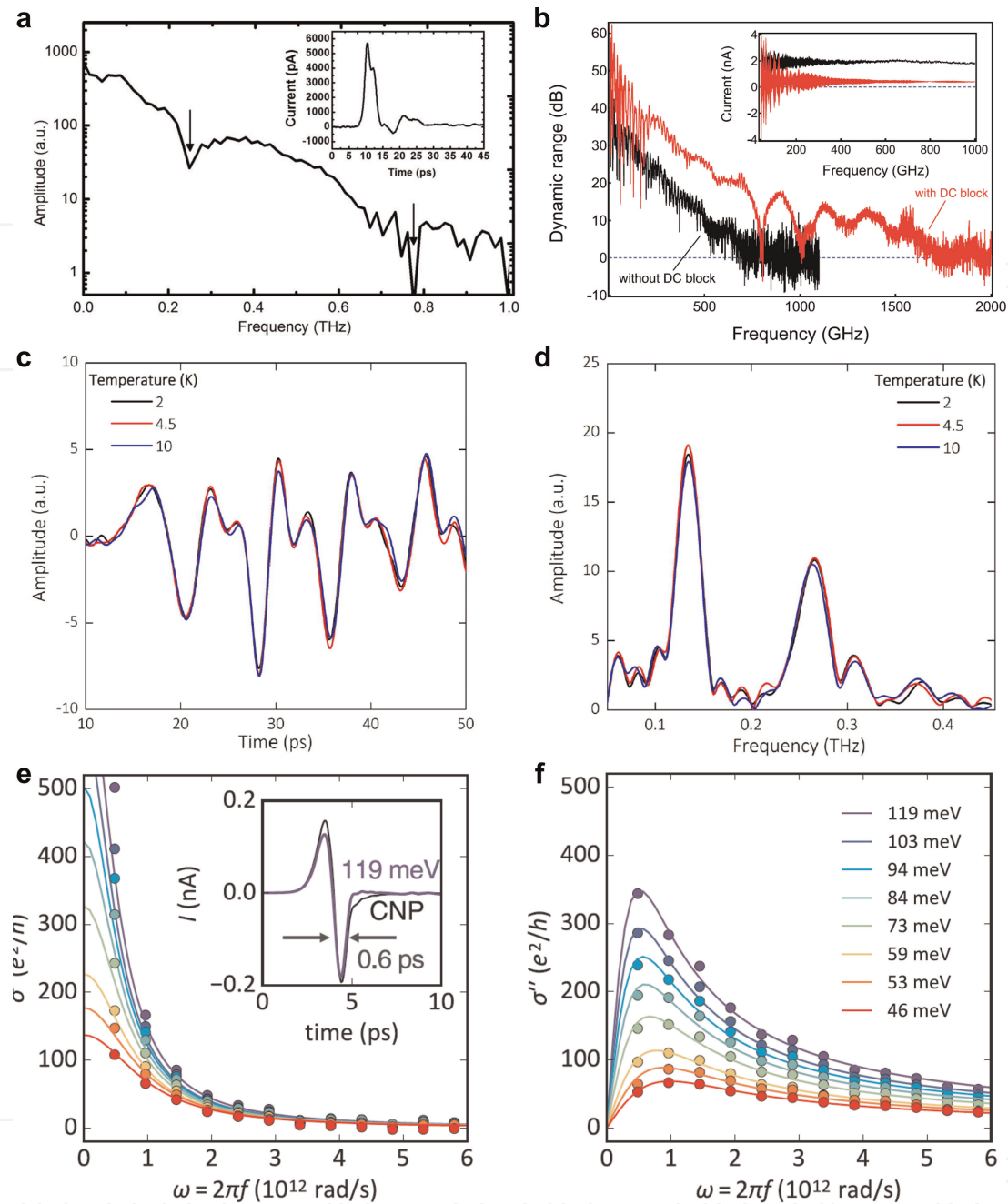


Figure 4. Examples of on-chip THz spectroscopy. (a) Transmission spectra of a Goubau waveguide device with a band-stop filter (a stub line fabricated on the Goubau line shown in Figure 2(d)). The dips with arrows indicate the band stop frequencies of 250 GHz (fundamental mode) and 780 GHz (third harmonic). The inset shows the time domain scan used to form the spectra in the main panel from a Fourier transform. This panel has been adapted from ref. [70]. (b) Amplitude spectra obtained for a coplanar waveguide device with and without a DC block (discontinuity in the central conductor). The inset shows the raw current measurement from which the amplitude spectra is calculated. This panel has been adapted from ref. [117]. (c) Time-domain data at different temperatures of a coplanar device with a 2DEG (AlGaAg/GaAs) mesa integrated within the centerline conductor. (d) Amplitude spectra of the Fourier transformed time-domain data in panel (c). Resonant peaks correspond to plasmon excitations in the gated (132 GHz and 264 GHz) and ungated (311 GHz) regions. Panels (c) and (d) have been adapted from ref. [118]. (e) Real part of the complex conductivity of a graphene heterostructure integrated within a coplanar transmission line device. The colored curves correspond to different Fermi energies labeled in the legend in panel (f). The solid lines are fits to the Drude model. The inset shows the time-domain data for two different Fermi energies. (f) The imaginary part of the complex conductivity of a graphene heterostructure. The solid lines are fits to the Drude model. Panels (e) and (f) have been adapted from ref. [119].

work. They investigated devices with and without a DC block (a gap in the centerline conductor) in a coplanar waveguide structure. The data (red) measured with a DC block show dips in the spectra due to interference of even and odd modes of the waveguide. The DC block enhances the bandwidth spectrometer and reduces unwanted DC leakage currents.

On-chip THz spectrometers have also been used to study plasmon excitations in clean 2DEG systems [118, 120, 121]. Wu et al. showed that plasmon excitations in an etched mesa of AlGaAs/GaAs could be electrically gated [118]. **Figure 4(c)** shows their time-domain data. Very prominent oscillations with different periods can be seen. The Fourier transform of the time-domain data is shown in **Figure 4(d)**. Three peaks are produced at frequencies of 132, 264, and 311 GHz. The lower frequencies coincide with the predicted plasmon frequency of the first and second mode for the gated region of the device. The third resonance agrees with the plasmon frequency expected for the ungated region.

One of the qualities of the on-chip system, as highlighted in the introduction, is the ability to probe materials below the diffraction limit. Clean exfoliated 2D materials are typically tens of microns on a side and are well-suited for investigation with on-chip spectroscopy. Gallagher et al. have probed the THz properties of a graphene heterostructure using a coplanar transmission line and LT-GaAs photoconductive switches [119]. They investigated the predicted quantum critical characteristics of graphene at low doping and its hydrodynamic properties at higher doping. The inset of **Figure 4(e)** displays their time-domain data at two different dopings. The main panels of **Figure 4(e-f)** show the optical conductivity (real and imaginary, respectively) calculated from the Fourier transform of the time-domain data for various Fermi energies corresponding to the legend shown in **Figure 4(f)**. The data follow the Drude formula closely, $\sigma = D_{gr}\pi^{-1}(\tau^{-1} - i\omega)^{-1}$ with the known Drude weight of graphene, $D_{gr} = 2(e/\hbar)^2 k_B T_e \log\left(2\cosh\left(m(2k_B T_e)^{-1}\right)\right)$ and τ the only fitting parameter. This data shows the Fermi liquid character of graphene at finite doping. The authors go on to extract the scattering rates for charge neutral graphene, finding support for quantum critical behavior in their linear dependence with temperature.

6. THz spectroscopy of liquids

In addition to solids, several research groups have incorporated reservoirs and microfluidic channels to perform spectroscopy on liquids. This could open up an avenue toward diagnostic devices for the detection of low-concentration biomolecules or investigations of chemical reactions *in-situ*.

Probably the most straightforward approach to investigating liquids is by fabricating a microfluidic channel or reservoir on the surface of the chip [73–81]. Swithenbank et al. has shown that a polydimethylsiloxane (PDMS) molded microfluidic channel can be plasma-bonded to the surface of a Goubau waveguide chip [74]. **Figure 5(a)** shows a model schematic of the device. A thin (6 μm) layer of benzocyclobutene is spun on the chip before the PDMS mold to electrically isolate the Goubau line from the liquid channel. Using this device, they measured the complex permittivity of several liquids in the THz regime including methanol, ethanol, propan-1-ol, butan-1-ol, hexan-1-ol, octan-1-ol, and mixtures of propan-2-ol/DI-H₂O. **Figure 5(b)** displays measurements on mixtures of propan-2-ol/DI-H₂O for different concentrations of DI-H₂O in 10% increments from red (0%) to purple (100%). The

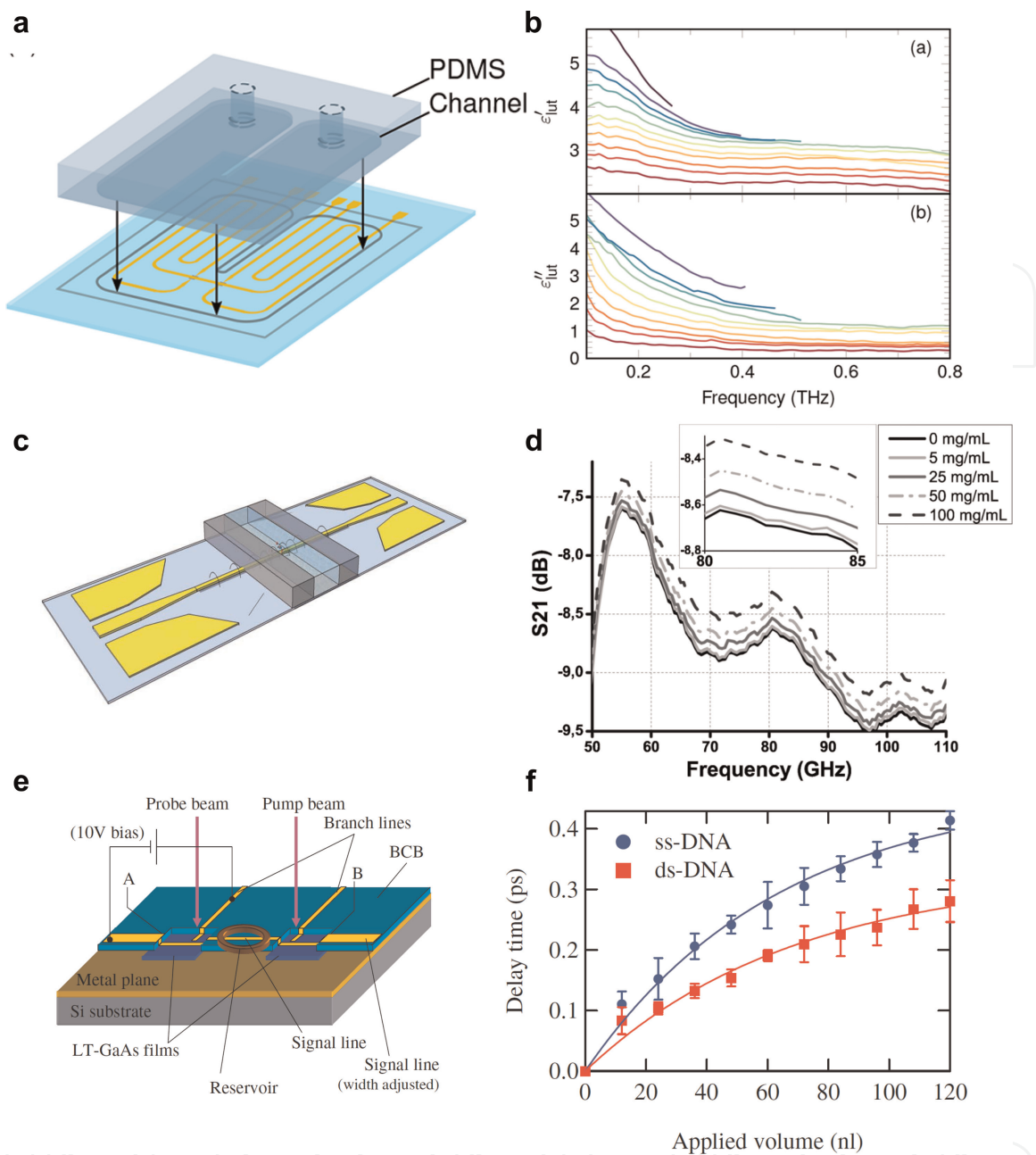


Figure 5. Examples of on-chip THz spectroscopy of liquids. (a) Model schematic of an on-chip spectrometer for measurements of liquids. A PDMS mold is plasma bonded to the surface of a Goubau line device. (b) Complex permittivity measured for various mixtures of propan-2-ol/DI-H₂O for different concentrations of DI-H₂O in 10% increments from red (0%) to purple (100%). Panels (a) and (b) have been adapted from ref. [74]. (c) Model schematic of an on-chip spectrometer for measurements of liquids. A silicon microfluidic channel is fabricated on the surface of a Goubau line device. (d) Transmission (S_{21}) measurements of various concentrations of BSA in DI water. Panels (c) and (d) have been adapted from ref. [75]. (e) Model schematic of an on-chip spectrometer for measurements of liquids. A reservoir made from SU-8 photoresist is created on the surface of a chip with a microstrip line. (f) THz pulse delay as a function of sample volumes of single-stranded (ss) and double-stranded DNA. The solid lines are fits to an exponential model. Panels (e) and (f) have been adapted from ref. [80].

complex permittivity can be seen to gradually increase with the percentage of DI-H₂O, as expected. One can also appreciate from the data that the bandwidth of the measurement decreases as the mixture becomes more absorbing. This highlights a design parameter of the spectrometer that is important. If greater bandwidth for a relatively absorbing substance is required, one can reduce the interaction volume

between the probing field and the measured liquid by shrinking the volume of the microfluidic channel.

Another example of this sort of device is given by Laurette et al. [75]. They also used a Goubau line device but instead of using photoconductive switches pumped with femtosecond lasers, they connected the chip to a high-frequency vector network analyzer with frequency bands of 0–110 GHz and 140–220 GHz. They measured mixtures of bovine Serum Albumin (BSA) in DI water and lysozyme in DI water at different concentrations to study hydration shell structure. **Figure 5(c)** shows a model schematic of the device consisting of a Goubau line fabricated on a pyrex borosilicate glass substrate. The microfluidic channel is created by deep reactive ion etching of silicon that is bonded to the glass substrate [81]. **Figure 5(d)** shows the measured transmission (S21) for various concentrations of BSA powders. The transmission amplitude is seen to increase with BSA concentration. They found a lower detectable sensitivity limit of the system of 5 mg/mL^2 for protein spectroscopy.

Kasai et al. have demonstrated THz pulse measurements of DNA solutions using an on-chip device consisting of a microstrip line fabricated on a silicon substrate, **Figure 5(e)** [80]. A sample reservoir with a diameter of $400 \text{ }\mu\text{m}$ and a height of $6.5 \text{ }\mu\text{m}$ was created from SU-8 photoresist. **Figure 5(f)** displays their results showing that the pulse delay tracks with the amount of single-stranded (ss) and double-stranded (ds) DNA samples. The pulse's propagation is exponentially delayed with increased sample volume and follows the expected trend of $t = t_{sat}[1 - \exp(-d/V)]$, where V is the sample volume, and t_{sat} and d are fitting parameters. The distinct difference between the single-stranded and double-stranded results paves the way for a diagnostic device for biomedical sciences.

Finally, highlighting the versatility of on-chip spectroscopy, Russel et al. [122] have presented measurements of various alcohols using a Goubau line fabricated on a flexible polyimide substrate wrapped around a quartz capillary (3 mm diameter with $10 \text{ }\mu\text{m}$ thick walls). Using this system they were able to measure the time-of-flight permittivities [123] of various alcohols. The measurement only provided relative approximations of the permittivities but the signal-to-noise ratio was found to be better than that obtained from free-space measurements of the same alcohols. The flexible substrate approach provides another degree-of-freedom in the design of on-chip systems.

7. Conclusions

This chapter has reviewed the history and common applications of on-chip THz time-domain spectroscopy. Free-space THz methods struggle to probe samples smaller than the diffraction limit. Still, several techniques have been developed to overcome this limit using apertures, sharp metal tips, and on-chip waveguides. Common designs include coplanar transmission lines and Goubau waveguides. Using photolithography and metallization, the circuit design has many freedoms, useful for signal routing, filtering, and even selecting the propagation mode of the electric field.

Using this technique, researchers have investigated electronic properties of materials in both the time and frequency domain. Time-domain data can show the evolution of a system with picosecond resolution. This has been used to show rapid phenomena, such as magnetoplasmon oscillations in GaAs/AlGaAs 2DEGs, ballistic carrier resonances in carbon nanotubes, and emission and relaxation characteristics of

a variety of photoconductive materials impinged by a femtosecond laser pulse. Frequency-domain data is calculated using a simple discrete Fourier transform of the time domain. This absorption spectra have been used to characterize on-chip band filters, assess the efficacy of DC blocks in the transmission line, and directly measure plasmon excitation frequencies in gated GaAs/AlGaAs. Additionally, the frequency-dependent complex conductivity of materials can be extracted from the THz spectra, enabling deep analysis of the scattering rates of electronic systems.

The modularity of chips allows microscopic liquid samples to be probed as well. Various designs for microfluidic cells have been developed, including reservoirs made of PDMS and photoresist, and channels etched into a silicon substrate, each fabricated atop a transmission line. These developments are especially useful for biomedical applications, as minimal sample size is necessary for comprehensive results. Studies include characterization of frequency bandwidth with various volumes of sample, determination of sensitivity to small samples of protein, and distinction between single-stranded and double-stranded DNA samples. The Goubau line design is also capable of fitting on a flexible substrate, demonstrating its versatility.

Terahertz spectroscopy has great potential in probing a realm of physics inaccessible by other techniques and applying it on a small-footprint chip opens up many interesting directions for future research. Spectroscopy on nanomaterials is one clear avenue for further development. THz spectral information could lead to a better understanding of complex ground states in 2D materials and heterostructures. One example is the recently discovered twisted heterostructures that present superconductivity such as twisted bilayer graphene. On-chip THz spectroscopy offers a method to probe these types of samples that are too small for free space measurements. The transmission spectra acquired could provide detailed tracking of spectral weight and sensitive investigation of the onset of interactions and correlations in these systems. Moreover, using on-chip spectroscopy with an optical pump would enable studies of quasiparticle dynamics and information on possible pairing mechanisms that are not well understood in twisted heterostructures.

Given the progress so far, another clear direction of development is the study of bioliquid samples on-chip. Many biomolecular motions present vibrational and rotational excitations in the THz spectrum. These excitations can serve as spectral fingerprints of the species for in-vitro diagnosis. Special attention will be needed on signal attenuation from water but careful adjustment of the interaction volume may lead to the detection of very low-concentration biomolecules in liquids. With advances in compact THz sources and detectors, new diagnostic devices with better sensitivity may be developed.

Acknowledgements

This material is based upon work supported by the National Science Foundation under Grant No. (2047509).

Conflict of interest

The authors declare no conflict of interest.

IntechOpen

IntechOpen


Author details

Randy M. Sterbentz and Joshua O. Island*

Department of Physics and Astronomy, University of Nevada Las Vegas, Las Vegas, USA

*Address all correspondence to: joshua.island@unlv.edu

IntechOpen

© 2023 The Author(s). Licensee IntechOpen. This chapter is distributed under the terms of the Creative Commons Attribution License (<http://creativecommons.org/licenses/by/3.0>), which permits unrestricted use, distribution, and reproduction in any medium, provided the original work is properly cited. 

References

- [1] Auston DH. Picosecond optoelectronic switching and gating in silicon. *Applied Physics Letters*. 1975; **26**(3):101-103
- [2] Auston DH, Cheung KP, Smith PR. Picosecond photoconducting Hertzian dipoles. *Applied Physics Letters*. 1984; **45**(3):284-286
- [3] Smith PR, Auston DH, Nuss MC. Subpicosecond photoconducting dipole antennas. *IEEE Journal of Quantum Electronics*. 1988; **24**(2):255-260
- [4] Fattinger C, Grischkowsky D. Point source terahertz optics. *Applied Physics Letters*. 1988; **53**(16):1480-1482
- [5] Fattinger C, Grischkowsky D. Terahertz beams. *Applied Physics Letters*. 1989; **54**(6):490-492
- [6] van Exter M, Fattinger C, Grischkowsky D. Terahertz time-domain spectroscopy of water vapor. *Optics Letters*. 1989; **14**(20):1128-1130
- [7] Huber R, Tauser F, Brodschelm A, Bichler M, Abstreiter G, Leitenstorfer A. How many-particle interactions develop after ultrafast excitation of an electron-hole plasma. *Nature*. 2001; **414**(6861):286-289
- [8] Dexheimer S, L. Terahertz Spectroscopy: Principles and Applications. Boca Raton: CRC Press; 2017
- [9] Porer M, Leierseder U, Ménard J-M, Dachraoui H, Mouchliadis L, Perakis IE, et al. Non-thermal separation of electronic and structural orders in a persisting charge density wave. *Nature Materials*. 2014; **13**(9):857-861
- [10] Hilton DJ, Prasankumar RP, Trugman SA, Taylor AJ, Averitt RD. On photo-induced phenomena in complex materials: Probing quasiparticle dynamics using infrared and far-infrared pulses. *Journal of the Physical Society of Japan*. 2006; **75**(1):011006
- [11] Averitt RD, Lobad AI, Kwon C, Trugman SA, Thorsmølle VK, Taylor AJ. Ultrafast conductivity dynamics in colossal magnetoresistance manganites. *Physical Review Letters*. 2001; **87**(1):017401
- [12] Aoki H. Novel Landau level laser in the quantum hall regime. *Applied Physics Letters*. 1986; **48**(9):559-560
- [13] Morimoto T, Hatsugai Y, Aoki H. Cyclotron radiation and emission in graphene. *Physical Review B*. 2008; **78**(7):073406
- [14] Wendler F, Malic E. Towards a tunable graphene-based Landau level laser in the terahertz regime. *Scientific Reports*. 2015; **5**(1):12646
- [15] Yang X, Zhao X, Yang K, Yueping Liu Y, Liu WF, Luo Y. Biomedical applications of terahertz spectroscopy and imaging. *Trends in Biotechnology*. 2016; **34**(10):810-824
- [16] Jing X, Plaxco KW, James S, Allen. Probing the collective vibrational dynamics of a protein in liquid water by terahertz absorption spectroscopy protein. *Science*. 2006; **15**(5):1175-1181
- [17] Dinca MP, Leca A, Apostol D, Mernea M, Calborean O, Mihailescu D, et al. Transmission thz time domain system for biomolecules spectroscopy. *Journal of Optoelectronics and Advanced Materials*. 2010; **12**(January 2010):110-114
- [18] Sczech R, Haring P, Bolvar. Thz spectroscopy of bovine serum albumin

solution using the long-range guided mode supported by thin liquid films. In: 2014 Conference on Lasers and Electro-Optics (CLEO)-Laser Science to Photonic Applications. San Jose, CA, USA: IEEE; 2014. pp. 1-2

[19] Yoon SA, Cha SH, Jun SW, Park SJ, Park J-Y, Lee S, et al. Identifying different types of microorganisms with terahertz spectroscopy. *Biomedical Optics Express*. 2020;**11**(1):406-416

[20] Fan S, He Y, Ung BS, Pickwell-MacPherson E. The growth of biomedical terahertz research. *Journal of Physics D: Applied Physics*. 2014;**47**(37):374009

[21] Pickwell E, Cole BE, Fitzgerald AJ, Pepper M, Wallace VP. In vivo study of human skin using pulsed terahertz radiation. *Physics in Medicine & Biology*. 2004;**49**(9):1595

[22] Wallace VP, Fitzgerald AJ, Shankar S, Flanagan N, Pye R, Cluff J, et al. Terahertz pulsed imaging of basal cell carcinoma ex vivo and in vivo. *British Journal of Dermatology*. 2004;**151**(2):424-432

[23] Yao X, Havenith M. Perspective: Watching low-frequency vibrations of water in biomolecular recognition by thz spectroscopy. *The Journal of Chemical Physics*. 2015;**143**(17):170901

[24] Cheon H, Yang H-j, Lee S-H, Kim YA, Son J-H. Terahertz molecular resonance of cancer DNA. *Scientific Reports*. 2016;**6**(1):1-10

[25] Niessen KA, Mengyang X, George DK, Chen MC, Adrian R, D'Amaré F, et al. Protein and RNA dynamical fingerprinting. *Nature Communications*. 2019;**10**(1):1-10

[26] Abbe E. Beiträge zur Theorie des Mikroskops und der mikroskopischen Wahrnehmung. *Archiv für Mikroskopische Anatomie*. 1873;**9**(1):413-468

[27] Lord Rayleigh FRSXXXI. Investigations in optics, with special reference to the spectroscope. *The London, Edinburgh, and Dublin Philosophical Magazine and Journal of Science*. 1879;**8**(49):261-274

[28] Novoselov KS, Geim AK, Morozov SV, Jiang D, Zhang Y, Dubonos SV, et al. Electric field effect in atomically thin carbon films. *Science*. 2004;**306**(5696):666-669

[29] Cao Y, Fatemi V, Fang S, Watanabe K, Taniguchi T, Kaxiras E, et al. Unconventional superconductivity in magic-angle graphene superlattices. *Nature*. 2018;**556**(7699):43-50

[30] Cao Y, Fatemi V, Demir A, Fang S, Tomarken SL, Luo JY, et al. Correlated insulator behaviour at half-filling in magic-angle graphene superlattices. *Nature*. 2018;**556**(7699):80-84

[31] Levene MJ, Korlach J, Turner SW, Foquet M, Craighead HG, Webb WW. Zero-mode waveguides for single-molecule analysis at high concentrations. *Science*. 2003;**299**(5607):682-686

[32] Moran-Mirabal JM, Craighead HG. Zero-mode waveguides: Sub-wavelength nanostructures for single molecule studies at high concentrations. *Methods*. 2008;**46**(1):11-17

[33] Zhu P, Craighead HG. Zero-mode waveguides for single-molecule analysis. *Annual Review of Biophysics*. 2012;**41**:269-293

[34] Adam AJL. Review of near-field terahertz measurement methods and

their applications. *Journal of Infrared, Millimeter, and Terahertz Waves*. 2011; **32**(8):976

[35] Kawano Y, Ishibashi K. An on-chip near-field terahertz probe and detector. *Nature Photonics*. 2008;**2**(10):618-621

[36] Moon K, Do Y, Park H, Kim J, Kang H, Lee G, et al. Computed terahertz near-field mapping of molecular resonances of lactose stereoisomer impurities with sub-attomole sensitivity. *Scientific Reports*. 2019;**9**(1): 1-8

[37] Synge EH, XXXVIII. A suggested method for extending microscopic resolution into the ultra-microscopic region. *The London, Edinburgh, and Dublin Philosophical Magazine and Journal of Science*. 1928;**6**(35):356-362

[38] Merz R, Keilmann F, Haug RJ, Ploog K. Nonequilibrium edge-state transport resolved by far-infrared microscopy. *Physical Review Letters*. 1993;**70**(5):651-653

[39] Hunsche S, Koch M, Brener I, Nuss MC. THz near-field imaging. *Optics Communications*. 1998;**150**(1): 22-26

[40] Nguyen TD, Vally Vardeny Z, Nahata A. Concentration of terahertz radiation through a conically tapered aperture. *Optics Express*. 2010;**18**(24): 25441-25448

[41] Rusina A, Durach M, Nelson KA, Stockman MI. Nanoconcentration of terahertz radiation in plasmonic waveguides. *Optics Express*. 2008; **16**(23):18576-18589

[42] Mitrofanov O, Brener I, Harel R, Wynn JD, Pfeiffer LN, West KW, et al. Terahertz near-field microscopy based on a collection mode detector.

Applied Physics Letters. 2000;**77**(22): 3496-3498

[43] Carnio BN, Elezzabi AY. Investigation of ultra-broadband terahertz generation from sub-wavelength lithium niobate waveguides excited by few-cycle femtosecond laser pulses. *Optics Express*. 2017;**25**(17): 20573-20583

[44] Bethe HA. Theory of diffraction by small holes. *Physical Review*. 1944;**66**(7-8):163-182

[45] Bouwkamp CJ. On the diffraction of electromagnetic waves by small circular disks and holes. *Philips Research Reports*. 1950;**5**:401-422

[46] Wessel J. Surface-enhanced optical microscopy. *JOSA B*. 1985;**2**(9): 1538-1541

[47] van der Valk NCJ, Planken PCM. Electro-optic detection of subwavelength terahertz spot sizes in the near field of a metal tip. *Applied Physics Letters*. 2002;**81**(9):1558-1560

[48] Chen H-T, Kersting R, Cho GC. Terahertz imaging with nanometer resolution. *Applied Physics Letters*. 2003;**83**(15):3009-3011

[49] Huber AJ, Keilmann F, Wittborn J, Aizpurua J, Hillenbrand R. Terahertz near-field Nanoscopy of Mobile carriers in single semiconductor Nanodevices. *Nano Letters*. 2008;**8**(11):3766-3770

[50] Zhang J, Chen X, Mills S, Ciavatti T, Yao Z, Mescall R, et al. Terahertz nanoimaging of graphene. *ACS Photonics*. 2018;**5**(7):2645-2651

[51] Yao Z, Semenenko V, Zhang J, Mills S, Zhao X, Chen X, et al. Photo-induced terahertz near-field dynamics of

graphene/InAs heterostructures. *Optics Express*. 2019;**27**(10):13611-13623

[52] von Ribbeck H-G, Brehm M, van der Weide DW, Winnerl S, Drachenko O, Helm M, et al. Spectroscopic THz near-field microscope. *Optics Express*. 2008; **16**(5):3430-3438

[53] Sprik R, Duling IN, Chi C-C, Grischkowsky D. Far infrared spectroscopy with subpicosecond electrical pulses on transmission lines. *Applied Physics Letters*. 1987;**51**(7): 548-550

[54] Matheisen C, Nagel M, Sawallich S. Coplanar stripline (CPS) emitter and transceiver microprobes for ultra-high bandwidth on-chip terahertz measurements. In: 2015 40th International Conference on Infrared, Millimeter, and Terahertz Waves (IRMMW-THz). Hong Kong, China: IEEE; 2015. pp. 1-3

[55] Saxler J, Gómez Rivas J, Janke C, Pellemans HPM, Haring Bolívar P, Kurz H. Time-domain measurements of surface plasmon polaritons in the terahertz frequency range. *Physical Review B*. 2004;**69**(15): 155427

[56] O'Hara JF, Averitt RD, Taylor AJ. Prism coupling to terahertz surface plasmon polaritons. *Optics Express*. 2005;**13**(16):6117-6126

[57] Auston DH, Johnson AM, Smith PR, Bean JC. Picosecond optoelectronic detection, sampling, and correlation measurements in amorphous semiconductors. *Applied Physics Letters*. 1980;**37**(4):371-373

[58] Auston D. Impulse response of photoconductors in transmission lines. *IEEE Journal of Quantum Electronics*. 1983;**19**(4):639-648

[59] Ketchen MB, Grischkowsky D, Chen TC, Chi C-C, Duling Iii IN, Halas NJ, et al. Generation of subpicosecond electrical pulses on coplanar transmission lines. *Applied Physics Letters*. 1986;**48**(12):751-753

[60] Paulter NG, Sinha DN, Gibbs AJ, Eisenstadt WR. Optoelectronic measurements of picosecond electrical pulse propagation in coplanar waveguide transmission lines. *IEEE Transactions on Microwave Theory and Techniques*. 1989;**37**(10):1612-1619

[61] Grischkowsky DR, Ketchen MB, Chi C-C, Duling IN, Halas NJ, Halbout J-M, et al. Capacitance free generation and detection of subpicosecond electrical pulses on coplanar transmission lines. *IEEE Journal of Quantum Electronics*. 1988;**24**(2):221-225

[62] Jacobsen RH, Karen Birkelund T, Holst PU, Jepsen, and SR Keiding. Interpretation of photocurrent correlation measurements used for ultrafast photoconductive switch characterization. *Journal of Applied Physics*. 1996;**79**(5):2649-2657

[63] Yanagi S, Onuma M, Kitagawa J, Kadoya Y. Propagation of terahertz pulses on coplanar strip-lines on low permittivity substrates and a spectroscopy application. *Applied Physics Express*. 2008;**1**(1):012009

[64] Prechtel L, Manus S, Schuh D, Wegscheider W, Holleitner AW. Spatially resolved ultrafast transport current in gas photoswitches. *Applied Physics Letters*. 2010;**96**(26):261110

[65] Jingbo W, Mayorov AS, Wood CD, Mistry D, Li L, Muchenje W, et al. Excitation, detection and electrostatic manipulation of terahertz-frequency range plasmons in a two-dimensional

- electron system. *Scientific Reports*. 2015; **5**(1):1-8
- [66] Wood CD, Mistry D, Li LH, Cunningham JE, Linfield EH, Davies AG. On-chip terahertz spectroscopic techniques for measuring mesoscopic quantum systems. *Review of Scientific Instruments*. 2013; **84**(8): 085101
- [67] Treizebré A, Bocquet B, Yansheng X, Bosisio RG. New thz excitation of planar goubau line. *Microwave and Optical Technology Letters*. 2008; **50**(11): 2998-3001
- [68] Gacemi D, Mangeney J, Laurant T, Lampin J-F, Akalin T, Blary K, et al. Thz surface plasmon modes on planar goubau lines. *Optics Express*. 2012; **20**(8):8466-8471
- [69] Zehar M, Moreno G, Chahadih A, Turer I, Ghaddar A, Akalin T. Low loss terahertz planar goubau line on high resistivity silicon substrate. In: 2013 13th Mediterranean Microwave Symposium (MMS). Saida, Lebanon: IEEE; 2013. pp. 1-3
- [70] Dazhang L, Cunningham J, Byrne MB, Khanna S, Wood CD, Burnett AD, et al. On-chip terahertz goubau-line waveguides with integrated photoconductive emitters and mode-discriminating detectors. *Applied Physics Letters*. 2009; **95**(9):092903
- [71] Hunter N, Mayorov AS, Wood CD, Russell C, Li L, Linfield EH, et al. On-Chip picosecond pulse detection and generation using graphene photoconductive switches. *Nano Letters*. 2015; **15**(3):1591-1596
- [72] Chi C, Gallagher W, Duling I, Grischkowsky D, Halas N, Ketchen M, et al. Subpicosecond optoelectronic study of superconducting transmission lines. *IEEE Transactions on Magnetics*. 1987; **23**(2):1666-1669
- [73] Amarloo H, Safavi-Naeini S. Enhanced on-chip terahertz vibrational absorption spectroscopy using evanescent fields in silicon waveguide structures. *Optics Express*. 2021; **29**(11): 17343-17352
- [74] Swithenbank M, Burnett AD, Russell C, Li LH, Davies AG, Linfield EH, et al. On-chip terahertz-frequency measurements of liquids. *Analytical Chemistry*. 2017; **89**(15): 7981-7987
- [75] Laurette S, Treizebre A, Elagli A, Hatirnaz B, Froidevaux R, Affouard F, et al. Highly sensitive terahertz spectroscopy in microsystem. *RSC Advances*. 2012; **2**(26):10064-10071
- [76] Park SJ, Cunningham J. Determination of permittivity of dielectric analytes in the terahertz frequency range using split ring resonator elements integrated with on-chip waveguide. *Sensors*. 2020; **20**(15): 4264
- [77] Tonouchi M. Terahertz microfluidic chip sensitivity-enhanced with a few arrays of meta atoms. In: *Optical Sensors*. Vancouver, British Columbia, Canada: Optica Publishing Group; 2018. p. SeTh4E-1
- [78] Serita K, Kobatake S, Tonouchi M. I-design terahertz microfluidic chip for attomolar-level sensing. *Journal of Physics: Photonics*. 2022; **4**(3):034005
- [79] Swithenbank M, Russell C, Burnett AD, Li LH, Linfield H, Davies G, et al. On-chip terahertz spectroscopy of liquid mixtures. In: 2015 40th International Conference on Infrared, Millimeter, and Terahertz Waves

(IRMMW-THz). Hong Kong, China: IEEE; 2015. pp. 1-3

[80] Kasai S, Tanabashi A, Kajiki K, Itsuji T, Kurosaka R, Yoneyama H, et al. Micro strip line-based on-chip terahertz integrated devices for high sensitivity biosensors. *Applied Physics Express*. 2009;2(6):062401

[81] Laurette S, Treizebre A, Bocquet B. Co-integrated microfluidic and THz functions for biochip devices. *Journal of Micromechanics and Microengineering*. 2011;21(6):065029

[82] Sato N, Kitagawa J, Kadoya Y. THz pulse propagation on microstrip discontinuities. *Journal of Infrared, Millimeter, and Terahertz Waves*. 2011; 32(5):666-672

[83] Dawood A, Wu JB, Wood CD, Li LH, Linfield EH, Davies AG, et al. Full-wave modelling of terahertz frequency plasmons in two-dimensional electron systems. *Journal of Physics D: Applied Physics*. 2019;52(21):215101

[84] Kadoya Y. THz wave propagation on strip lines: Devices, properties, and applications. In: 2007 19th International Conference on Applied Electromagnetics and Communications. Dubrovnik, Croatia: IEEE; 2007. pp. 1-4

[85] Ohta N, Yanagi S, Onuma M, Kitagawa J, Kadoya Y. Propagation of terahertz pulses on polymer-based coplanar striplines. In: 2008 Asia-Pacific Microwave Conference. Hong Kong, China: IEEE; 2008. pp. 1-4

[86] Hejase JA, Paladhi PR, Chahal PP. Terahertz characterization of dielectric substrates for component design and nondestructive evaluation of packages. *IEEE Transactions on Components, Packaging and Manufacturing Technology*. 2011;1(11):1685-1694

[87] Song H-J. Packages for terahertz electronics. *Proceedings of the IEEE*. 2017;105(6):1121-1138

[88] Fernandez N, Zimmermann P, Zechmann P, Wörle M, Kienberger R, Holleitner A. Toward femtosecond electronics up to 10 THz. In: *Ultrafast Phenomena and Nanophotonics XXIII*. Vol. 10916. International Society for Optics and Photonics; 2019. p. 109160R

[89] Russell C, Wood CD, Dazhang L, Burnett AD, Li LH, Linfield EH, et al. Increasing the bandwidth of planar on-chip THz devices for spectroscopic applications. In: 2011 International Conference on Infrared, Millimeter, and Terahertz Waves. Houston, TX, USA. pp. 1, 2011-3

[90] Russell C, Wood CD, Burnett AD, Li L, Linfield EH, Giles Davies A, et al. Spectroscopy of polycrystalline materials using thinned-substrate planar Goubau line at cryogenic temperatures. *Lab on a Chip*. London, United Kingdom: Royal Society of Chemistry; 2013;13(20): 4065-4070

[91] Piao Z, Tani M, Sakai K. Carrier dynamics and terahertz radiation in photoconductive antennas. *Japanese Journal of Applied Physics*. 2000;39(1R): 96

[92] Russell C. Broadband on-chip terahertz spectroscopy. [Phd thesis] University of Leeds. 2013.

[93] Island JO, Kissin P, Schalch J, Cui X, Haque SRU, Potts A, et al. On-chip terahertz modulation and emission with integrated graphene junctions. *Applied Physics Letters*. 2020;116(16):161104

[94] Gupta S, Whitaker JF, Mourou GA. Ultrafast carrier dynamics in III-V semiconductors grown by molecular-beam epitaxy at very low substrate

- temperatures. *IEEE Journal of Quantum Electronics*. 1992;**28**(10):2464-2472
- [95] Shaner EA, Lyon SA. Picosecond time-resolved two-dimensional ballistic electron transport. *Physical Review Letters*. 2004;**93**(3):037402
- [96] Zhong Z, Gabor NM, Sharping JE, Gaeta AL, McEuen PL. Terahertz time-domain measurement of ballistic electron resonance in a single-walled carbon nanotube. *Nature Nanotechnology*. 2008;**3**(4):201-205
- [97] McIver JW, Schulte B, Stein F-U, Matsuyama T, Jotzu G, Meier G, et al. Light-induced anomalous hall effect in graphene. *Nature Physics*. 2019;**16**:1-4
- [98] Erhard N, Seifert P, Prechtel L, Hertenberger S, Karl H, Abstreiter G, et al. Ultrafast photocurrents and THz generation in single InAs-nanowires. *Annalen der Physik*. 2013;**525**(1-2): 180-188
- [99] Kastl C, Karnetzky C, Brenneis A, Langrieger F, Holleitner A. Topological insulators as ultrafast Auston switches in on-chip THz-circuits. *IEEE Journal of Selected Topics in Quantum Electronics*. 2017;**23**(4):1-5
- [100] Kastl C, Karnetzky C, Karl H, Holleitner AW. Ultrafast helicity control of surface currents in topological insulators with near-unity fidelity. *Nature Communications*. 2015;**6**(1):6617
- [101] Seifert P, Vaklinova K, Kern K, Burghard M, Holleitner A. Surface state-dominated photoconduction and THz generation in topological Bi₂Te₂Se nanowires. *Nano Letters*. 2017;**17**(2): 973-979
- [102] Zimmermann P, Holleitner AW. On-site tuning of the carrier lifetime in silicon for on-chip THz circuits using a focused beam of helium ions. *Applied Physics Letters*. 2020;**116**(7):073501
- [103] Prechtel L, Song L, Schuh D, Ajayan P, Wegscheider W, Holleitner AW. Time resolved ultrafast photocurrents and terahertz generation in freely suspended graphene. *Nature Communications*. 2012;**3**(1):1-7
- [104] Brenneis A, Schade F, Drieschner S, Heimbach F, Karl H, Garrido JA, et al. THz-circuits driven by photo-thermoelectric, gate-tunable graphene-junctions. *Scientific Reports*. 2016;**6**(1): 35654
- [105] Parzinger E, Hetzl M, Wurstbauer U, Holleitner AW. Contact morphology and revisited photocurrent dynamics in monolayer MoS₂. *Npj 2D. Materials and Applications*. 2017;**1**(1):1-8
- [106] Prechtel L, Song L, Manus S, Schuh D, Wegscheider W, Holleitner AW. Time-resolved picosecond photocurrents in contacted carbon nanotubes. *Nano Letters*. 2011;**11**(1):269-272
- [107] Prechtel L, Padilla M, Erhard N, Karl H, Abstreiter G, Anna Fontcuberta I, et al. Time-resolved photoinduced thermoelectric and transport currents in GaAs nanowires. *Nano Letters*. 2012;**12**(5):2337-2341
- [108] Karnetzky C, Zimmermann P, Trummer C, Sierra CD, Wörle M, Kienberger R, et al. Towards femtosecond on-chip electronics based on plasmonic hot electron nano-emitters. *Nature Communications*. 2018;**9**(1):2471
- [109] Th Gerrits HAM, Van Den Berg J, Hohlfeld LB, Rasing T. Ultrafast precessional magnetization reversal by picosecond magnetic field pulse shaping. *Nature*. 2002;**418**(6897):509-512

- [110] Garzon S, Ye L, Webb RA, Crawford TM, Covington M, Kaka S. Coherent control of nanomagnet dynamics via ultrafast spin torque pulses. *Physical Review B*. 2008;**78**(18): 180401
- [111] Wilson RB, Yang Y, Gorchon J, Lambert C-H, Salahuddin S, Bokor J. Electric current induced ultrafast demagnetization. *Physical Review B*. 2017;**96**(4):045105
- [112] Wang Z, Pietz M, Walowski J, Förster A, Lepsa MI, Münzenberg M. Spin dynamics triggered by subterahertz magnetic field pulses. *Journal of Applied Physics*. 2008; **103**(12):123905
- [113] Yang Y, Wilson RB, Gorchon J, Lambert C-H, Salahuddin S, Bokor J. Ultrafast magnetization reversal by picosecond electrical pulses. *Science Advances*. 2017;**3**(11):e1603117
- [114] Jhuria K, Hohlfeld J, Pattabi A, Martin E, Cordova AYA, Shi X, et al. Spin-orbit torque switching of a ferromagnet with picosecond electrical pulses. *Nature Electronics*. 2020;**3**(11): 680-686
- [115] Polley D, Pattabi A, Rastogi A, Jhuria K, Diaz E, Singh H, et al. Picosecond spin-orbit torque induced coherent magnetization switching in a ferromagnet. arXiv preprint arXiv: 2211.08266. 2022
- [116] Kato YK, Myers RC, Gossard AC, Awschalom DD. Current-induced spin polarization in strained semiconductors. *Physical Review Letters*. 2004;**93**(17): 176601
- [117] Yoshioka K, Kumada N, Muraki K, Hashisaka M. On-chip coherent frequency-domain thz spectroscopy for electrical transport. *Applied Physics Letters*. 2020;**117**(16): 161103
- [118] Jingbo W, Mayorov AS, Wood CD, Mistry D, Li L, Muchenje W, et al. Excitation, detection, and electrostatic manipulation of terahertz-frequency range plasmons in a two-dimensional electron system. *Scientific Reports*. 2015; **5**(1):15420
- [119] Gallagher P, Yang C-S, Lyu T, Tian F, Kou R, Zhang H, et al. Quantum-critical conductivity of the Dirac fluid in graphene. *Science*. 2019;**364**(6436): 158-162
- [120] Jingbo W, Sydoruk O, Mayorov AS, Wood CD, Mistry D, Li L, et al. Time-domain measurement of terahertz frequency magnetoplasmon resonances in a two-dimensional electron system by the direct injection of picosecond pulsed currents. *Applied Physics Letters*. 2016; **108**(9):091109
- [121] Shaner EA, Lyon SA. Time-resolved impulse response of the magnetoplasmon resonance in a two-dimensional electron gas. *Physical Review B*. 2002;**66**(4):041402
- [122] Russell C, Swithenbank M, Wood CD, Burnett AD, Li L, Linfield EH, et al. Integrated on-chip thz sensors for fluidic systems fabricated using flexible polyimide films. *IEEE Transactions on Terahertz Science and Technology*. 2016;**6**(4):619-624
- [123] Mittleman DM, Hunsche S, Boivin L, Nuss MC. T-ray tomography. *Optics Letters*. 1997;**22**(12):904-906